

Annealing temperature dependance of magnetic properties and magneto-impedance effect in CoZrB alloys

K. Zhang^a, D.W. Zhou^a, B. Han^a, Z. Lv^b, X.C. Xun^a, X.B. Du^a, Y.Q. Liu^b,
B. Yao^{a,c,*}, T. Zhang^a, B.H. Li^c, D. Wang^a

^a Department of Physics, Jilin University, No. 2519, Jiefang Road, Changchun 130023, PR China

^b Center for Condensed-Matter Science and Technology, Harbin University of Technology,
Harbin 150001, PR China

^c Key Laboratory of Excited State Process, Chinese Academy of Sciences, Changchun Institute of Optics, Fine Mechanics and Physics,
Chinese Academy of Sciences, Changchun 130022, PR China

Received 16 March 2007; received in revised form 1 October 2007; accepted 1 October 2007

Available online 5 October 2007

Abstract

The influence of conventional annealing on the magnetic properties and the magneto-impedance (MI) effect of Co₇₂Zr₈B₂₀ alloys has been intensively studied in this paper. The as-quenched Co₇₂Zr₈B₂₀ ribbon is identified to be amorphous alloy. After Co₇₂Zr₈B₂₀ being annealed at 495 °C for 10 min, there is almost no change in the XRD pattern. When the annealing temperature (T_a) reaches 540 °C, a diffraction peak representing some crystalline phase appears. After the sample being annealed at 630 °C, Co, Zr and B₁₂Zr crystalline phase are formed in the alloy. Magnetic measurements reveal that the as-quenched Co₇₂Zr₈B₂₀ possesses smaller coercivity, higher permeability and larger saturation magnetization. With the increasing annealing temperature, the soft magnetic properties of the sample greatly deteriorate. The study on the MI ratio ($\Delta Z/Z(\%)$) versus external magnetic field curves indicates that the MI behavior changes from single-peak to double-peak shape when T_a increases from 495 to 540 °C. The most drastic MI ratio about 90% is obtained in the as-quenched Co₇₂Zr₈B₂₀ at 1110 kHz. The mechanism of thermal treatment affecting the magnetic properties and the MI effect in Co₇₂Zr₈B₂₀ alloys will be discussed in this paper.

© 2007 Elsevier B.V. All rights reserved.

Keywords: Amorphous materials; X-ray diffraction; Magnetic measurements; Anisotropy

1. Introduction

The magneto-impedance (MI) effect, which has been observed in a lot of magnetic materials, is the large variation of impedance in soft magnetic materials induced by a dc magnetic field in the presence of a certain frequency ac current. Since its discovery in 1994 [1,2], it has attracted special attention due to the potential applications in technological field [3,4] and has been investigated in a variety of Fe- and Co-based amorphous ribbons [5–7], thin films [8–10], multi-layer films with sandwiched structures [11–14] and wires [15–17]. The origin of MI effect lies in the change in the permeability of the ferromagnetic conductor by the application of the external static magnetic field. This phenomenon has been understood on the basis of classical

electrodynamics through the relation between skin depth and permeability [18,19].

Many research results have confirmed that the MI effect is very sensitive to the composition, sample shape, stress and annealing conditions. In amorphous materials, the MI effect can be optimized by subjecting the materials to thermal and stress treatments and inducing transverse anisotropy. Thermal treatments can modify the structure and properties of the amorphous magnetic materials through stress release and structural relaxation of the amorphous phase or through the growth of the crystallized layer at the sample surface [20]. According to some previous studies [21–23], material which displays a large and sensitive MI effect has to comply as much as possible with the following three conditions: (i) it has to display good soft magnetic properties, i.e. high permeability and low coercive force, and (ii) it has to have an appropriate domain structure, usually transverse domain structure for ribbon (in-plane, perpendicular to the ribbon axis and to the applied magnetic field as well)

* Corresponding author. Fax: +86 431 84627031.
E-mail address: binyao@mail.jlu.edu.cn (B. Yao).

and circumferential domain structure for wire. (iii) Most materials possess a very small negative magnetostriction. MI effect of more than 100% has been obtained in many wire and multi-layer system. However, since the microstructure of material is complex and the annealing temperature and time are not easy to master and control, it is difficult to obtain materials with all the mentioned conditions to be satisfied.

Inoue et al. [24] have found that Co-based amorphous alloys with glass transition and supercooled liquid region are formed in Co–Fe–M–B (M = Zr, Nb) systems and exhibit good soft magnetic properties with high permeability. In their work [24], $\text{Co}_{72-x}\text{Fe}_x\text{Zr}_8\text{B}_{20}$ ($x = 0\text{--}21$ at.%) alloys, with permeability of 5500–18,300 in the frequency range of 1–10³ kHz and low magnetostriction between -1.5×10^{-6} and $+10 \times 10^{-6}$ including zero, have been intensively studied. Based on their reports, we prepared $\text{Co}_{72-x}\text{Fe}_x\text{Zr}_8\text{B}_{20}$ ($x = 0, 2, 5, 7$ at.%) (CFZB) amorphous alloys and found that the as-quenched Fe-free CFZB exhibits the best MI effect [25], which is attributed to its largest permeability determined by the domain structure of the material, small resistivity and a slightly negative magnetostriction. In conformity to our research results, we carried out thermal treatments on the $\text{Co}_{72}\text{Zr}_8\text{B}_{20}$ alloys. The aim of this paper is to investigate the influence of thermal treatment on the magnetic properties and the MI effect of $\text{Co}_{72}\text{Zr}_8\text{B}_{20}$ ribbons.

2. Experimental procedures

The $\text{Co}_{72}\text{Zr}_8\text{B}_{20}$ ribbons, made by melt-spinning technique in an argon atmosphere with the roll speed of about 25 m/s, had reasonably uniform thickness (35–40 μm) and width (1.5 mm). Some of the ribbons were annealed at the temperature of 495, 540 and 630 °C for 10 min, respectively, in a high vacuum condition to the order of 10^{-3} Pa, then cooled naturally at the room temperature. The state of the ribbons was examined by X-ray diffraction technique. Magnetization measurements at room temperature were carried out using a vibrating sample magnetometer (VSM). Solartron 1260 Impedance Analyzer was used for impedance measurements.

A four-probe ac technique was used to measure the magnitude Z of the magnetoimpedance as function of the field H applied along the ribbon length (about 50 mm), i.e. parallel to the ac measuring current. The current amplitude was kept constant ($I = 3$ mA) and frequency f was between 310 and 1110 kHz. The external field was generated by a solenoid with axis perpendicular to the Earth's magnetic field to allow field variation from 0 to 70 Oe.

3. Results and discussion

The X-ray diffraction patterns for the as-quenched and annealed $\text{Co}_{72}\text{Zr}_8\text{B}_{20}$ ribbons are plotted in Fig. 1. The XRD of the as-quenched $\text{Co}_{72}\text{Zr}_8\text{B}_{20}$ ribbon is shown in Fig. 1(a), which exhibits one broad diffused diffraction peak. This indicates that the as-quenched sample is amorphous alloy. After $\text{Co}_{72}\text{Zr}_8\text{B}_{20}$ being annealed at 495 °C, there is still no crystalline phase existing in the XRD pattern (see Fig. 1(b)). When the annealing temperature (T_a) reaches 540 °C, an obvious diffraction peak representing some crystalline phase appears, as observed in Fig. 1(c). After the sample being annealed at 630 °C, as shown in Fig. 1(d), Co, Zr and B₁₂Zr crystalline phase are formed.

For better understanding of the magnetic properties of $\text{Co}_{72}\text{Zr}_8\text{B}_{20}$, longitudinal hysteresis loops of the as-quenched and annealed samples have been studied and plotted in Fig. 2.

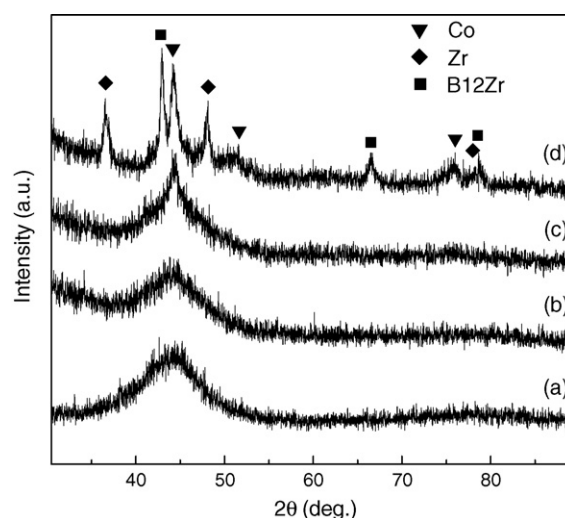


Fig. 1. X-ray diffraction patterns of $\text{Co}_{72}\text{Zr}_8\text{B}_{20}$ alloys in the as-quenched state (a), and annealed at 495 (b), 540 (c) and 630 °C (d) for 10 min.

The field of high magnitude was generated at these measurements. As seen from Fig. 2 that the as-quenched $\text{Co}_{72}\text{Zr}_8\text{B}_{20}$ exhibits excellent soft magnetic properties and only needs a comparatively small field to saturate the sample. The almost linear longitudinal hysteresis loop with zero remanence indicates a transverse magnetic structure. After the sample being annealed at 495 °C, although there is no evident change in the XRD pattern, the inner structure of the ribbon is modified to some extent, leading to the middle part of the hysteresis loop of the sample slightly deflecting from the original direction (shown in Fig. 2), which means an increase in the anisotropy value. When T_a increases from 495 to 540 °C, the hysteresis loop changes little. Anhysteretic portion of the magnetization is due to rotation of magnetic moment, which is the basic process for the above three almost linear hysteresis loops. However, due to the complexity of the domain structures and the domain wall motion in an applied field, as well as the lack of a good technique for characterization, the microstructures of $\text{Co}_{72}\text{Zr}_8\text{B}_{20}$ still need to be further studied. After $\text{Co}_{72}\text{Zr}_8\text{B}_{20}$ being annealed at 630 °C for 10 min, the central part of the hysteresis loop changes from nearly linear shape to “s” shape. Wide hysteresis with large remanence to saturation ratio after highest temperature annealing is a characteristic of a nearly longitudinal domain structure. The coercive force of the sample goes up greatly, which is attributed to the crystallization of the sample.

Coercivity (H_c) of the as-quenched and annealed $\text{Co}_{72}\text{Zr}_8\text{B}_{20}$ ribbons evaluated from the hysteresis loops is shown in Table 1. It is found that coercivity for the as-quenched $\text{Co}_{72}\text{Zr}_8\text{B}_{20}$ is the smallest among all the studied alloys. With the increasing annealing temperature H_c goes up notably, indicating the deterioration of soft magnetic properties. When the annealing temperature reaches 630 °C, H_c reaches 925 Oe, suggesting that the sample becomes magnetic hard. Moreover, relative permeability (μ') and saturation magnetization (M_s) of the $\text{Co}_{72}\text{Zr}_8\text{B}_{20}$ alloys have been estimated from the hysteresis loops. Annealing temperature dependance of the two parameters is shown in Fig. 3(a) and (b), respectively. It can be seen clearly from

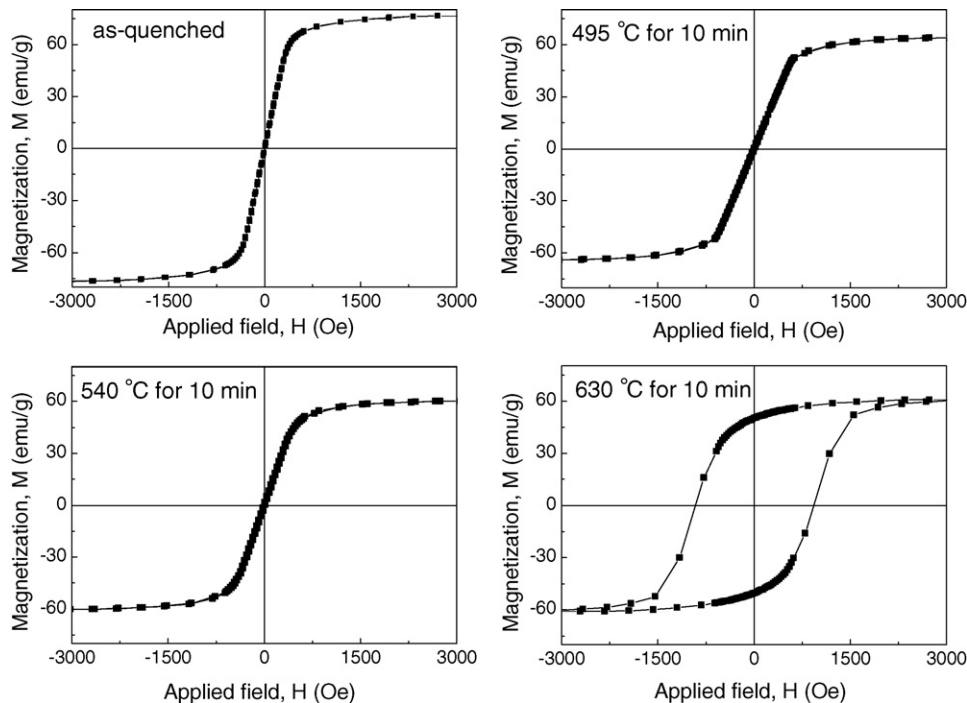


Fig. 2. Longitudinal hysteresis loops of the as-quenched and annealed Co₇₂Zr₈B₂₀ ribbons.

Fig. 3 that both μ' and M_s show the decreasing tendency with the increasing T_a . All these facts further confirmed the decline of soft magnetic properties with the increase of annealing temperature. The impedance Z of Co₇₂Zr₈B₂₀ as a function of the external longitudinal dc field was measured at $f=310, 510, 810, 910$ and 1110 kHz. The MI ratio $\Delta Z/Z(\%)$ denotes $[Z(H) - Z(H_{\max})]/Z(H_{\max})$, in which $Z(H_{\max})$ is the impedance value under the maximum magnetic field of 66 Oe. Fig. 4 shows the field dependence of MI ratio of the as-quenched and annealed Co₇₂Zr₈B₂₀ at 910 kHz. It is found that the MI curves show different changing tendency with the applied magnetic field. In general, there are two types of MI curves, one is single-peak curve, the other is the double-peak curve. A single-peak curve typically is a characteristic of the longitudinal anisotropy, however, for lower frequencies at appropriate ac current magnitude it can be seen in systems with a transverse anisotropy due to domain wall movements [18,19]. In the present work, the MI curve for the as-quenched Co₇₂Zr₈B₂₀ alloy belongs to this case. The largest MI value observed in the sample is about 80%. For annealing at 495 °C, the MI curve also shows single-peak behavior but the maximum MI value decreases to 43%. The decline of the MI response in the annealed ribbon is attributed to the deterioration of the soft magnetic properties caused by the

change of microstructure of the sample with thermal treatments. After Co₇₂Zr₈B₂₀ being annealed at 540 °C, when coercivity increases with annealing temperature, the wall movements do not occur and the MI effect is due to the magnetization rotation with two symmetrical peaks for a transverse anisotropy [18,19].

Table 1
Coercive field H_c of as-quenched and annealed Co₇₂Zr₈B₂₀ alloys

Specimen	H_c (Oe)
Sample A (as-quenched)	2.27
Sample B (annealed at 495 °C for 10 min)	5.13
Sample C (annealed at 540 °C for 10 min)	11.45
Sample D (annealed at 630 °C for 10 min)	925.27

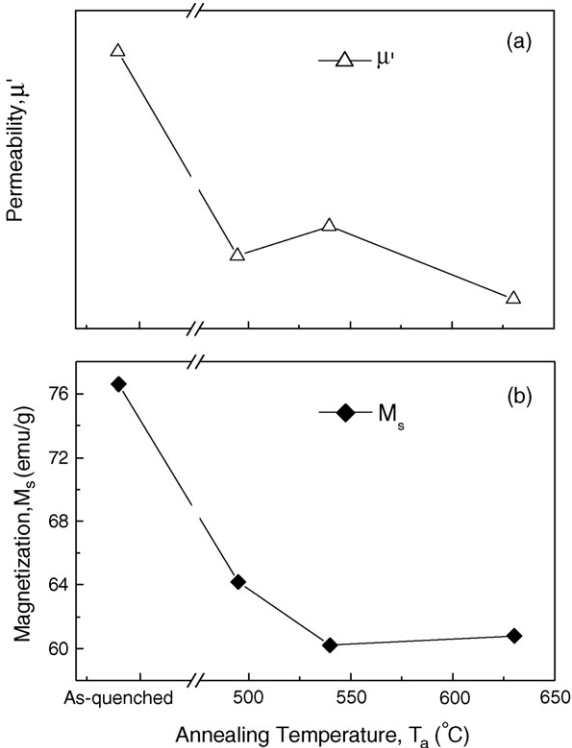


Fig. 3. Annealing temperature (T_a) dependence of permeability μ' (a) and saturation magnetization M_s (b).

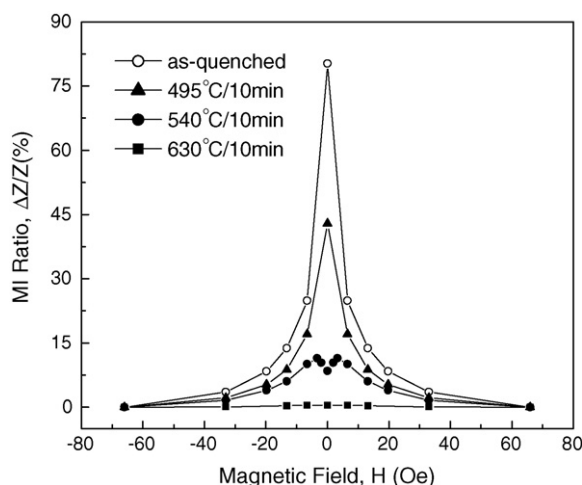


Fig. 4. The curves of MI ratio ($\Delta Z/Z(\%)$) versus longitudinal magnetic field (H) at the frequency of 910 kHz for the as-quenched and annealed $\text{Co}_{72}\text{Zr}_{18}\text{B}_{10}$ ribbons.

According to previous studies [26–28], the manipulation of the magnetic anisotropy of the ribbon increases the magnitude of the effect. In our case, as the deterioration of soft magnetic properties play the dominant role, the MI effect decreases greatly. When T_a reaches 630 °C, no obvious MI effect is observed due to the magnetic hardening of the material. To be mentioned, the field scale for impedance does not correspond to the transverse anisotropy (more than 700 Oe from Fig. 2), which still remains to be further studied.

The changes of the maximum MI ratio ($\Delta Z/Z(\%)_{\text{max}}$) with frequencies for the as-quenched and annealed $\text{Co}_{72}\text{Zr}_{18}\text{B}_{10}$ are plotted in Fig. 5. It can be noted that $\Delta Z/Z(\%)_{\text{max}}$ goes up with frequency for the sample in the as-quenched state and annealed at 495 °C. For $\text{Co}_{72}\text{Zr}_{18}\text{B}_{10}$ annealed at 540 °C, $\Delta Z/Z(\%)_{\text{max}}$ increases with frequency at beginning, reaching the maximum value of 11% at 910 kHz, and then slightly goes down. Besides, it can be seen from Fig. 5 that no MI response is obtained in the sample annealed at 630 °C at any of the measuring frequencies. Many previous research results have confirmed that

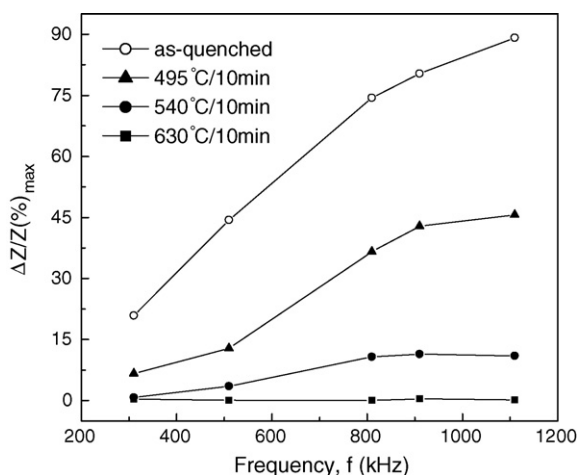


Fig. 5. The dependence of the maximum MI ratio ($\Delta Z/Z(\%)_{\text{max}}$) on the frequency for the as-quenched and annealed $\text{Co}_{72}\text{Zr}_{18}\text{B}_{10}$ ribbons.

maximum MI ratio increases with increasing driving frequency, and then decreases when frequency exceeds some a critical value [29,30]. The decrease of MI effect at high frequencies is due to the strong suppression of the domain wall movement by eddy current effect, which causes an extreme decrease of permeability [29,31–33]. As the highest frequency can only reach 1110 kHz under our experimental conditions, we are unable to give full $\Delta Z/Z(\%)_{\text{max}}$ –frequency curves for $\text{Co}_{72}\text{Zr}_{18}\text{B}_{10}$ in the as-quenched state and annealed at 495 °C. In many cases, with increasing frequency the MI effect increases due to involvement of the rotational processes. The failure to observe this is often related with an experimental setup where the length of the sample influences greatly the results providing a constant inductive contribution. Besides, as shown in Fig. 5, $\Delta Z/Z(\%)_{\text{max}}$ decreases with the increasing annealing temperature at any frequency. The as-quenched sample exhibits the most evident MI effect, especially as large as 90% at 1110 kHz, which is much higher than that obtained in other Co-based as-quenched alloys [34–36]. Both the drastic MI effect and the most prominent frequency response are due to the excellent soft magnetic properties of the sample, i.e. small coercivity, large saturation magnetization and high permeability determined by the domain structure of the material. Moreover, the as-quenched $\text{Co}_{72}\text{Zr}_{18}\text{B}_{10}$ possesses the highest field sensitivity at any frequency, as large as 18%/Oe at 1110 kHz, making the alloy more promising for technical applications in different kinds of high sensitivity micromagnetic sensors.

4. Conclusions

Thermal treatments in a high vacuum condition were performed on the amorphous $\text{Co}_{72}\text{Zr}_{18}\text{B}_{10}$ ribbons at 495, 540 and 630 °C for 10 min, respectively. After $\text{Co}_{72}\text{Zr}_{18}\text{B}_{10}$ being annealed at 495 °C, there is still no crystalline phase existing in the XRD pattern. When the annealing temperature reaches 540 °C, fcc-Co phase appears. After the sample being annealed at 630 °C, Co, Zr and B_{12}Zr crystalline phase are formed. The specimen in the as-quenched state possesses the best soft magnetic properties, i.e. smaller coercivity, higher permeability and larger saturation magnetization, and shows the maximum MI ratio of 90% at 1110 kHz and the field sensitivity of 18%/Oe. With the increasing annealing temperature the anisotropy value increases, and also the soft magnetic properties of $\text{Co}_{72}\text{Zr}_{18}\text{B}_{10}$ gradually deteriorate due to the change of microstructure, which leads to the reduction in the MI effect. Moreover, after the sample being annealed at 540 °C, MI curve changes from single-peak to double-peak behavior due to magnetization rotation. After $\text{Co}_{72}\text{Zr}_{18}\text{B}_{10}$ being annealed at 630 °C, no obvious MI effect is observed due to the magnetic hardening of the material.

Acknowledgements

This work is supported by the National Natural Science Foundation (grant no. 50472003), Doctoral Foundation of Education Ministry of China (grant no. 20040183063) and Creative Fund of Jilin University.

References

- [1] R.S. Beach, A.E. Berkowitz, *J. Appl. Phys.* 76 (1994) 6209.
- [2] L.V. Panina, K. Mohri, *Appl. Phys. Lett.* 65 (1994) 1189.
- [3] K. Mohri, T. Uchiyama, L.P. Shen, C.M. Cai, L.V. Panina, *Sens. Actuators A* 91 (2001) 85.
- [4] K. Mohri, T. Uchiyama, L.P. Shen, C.M. Cai, L.V. Panina, Y. Honkura, M. Yamamoto, *IEEE Trans. Magn.* 38 (2002) 3063.
- [5] M. Coisson, P. Tiberto, F. Vinai, S.N. Kane, *Sens. Actuators A* 106 (2003) 199.
- [6] J. He, H.Q. Guo, B.G. Shen, K.Y. He, H.W. Zhang, *Mater. Sci. Eng. A* 304–306 (2001) 988.
- [7] S.K. Pal, N.B. Manik, A. Mitra, *Mater. Sci. Eng. A* 415 (2006) 195.
- [8] R.L. Sommer, C.L. Chien, *Appl. Phys. Lett.* 67 (1995) 3346.
- [9] X.D. Li, W.Z. Yuan, Z.J. Zhao, X.Z. Wang, J.Z. Ruan, X.L. Yang, *J. Magn. Magn. Mater.* 279 (2004) 429.
- [10] M.M. Tehranchi, S.M. Mohseni, *J. Optoelectron. Adv. Mater.* 6 (2004) 667.
- [11] T. Morikawa, Y. Nishibe, H. Yamadera, Y. Nonomura, M. Takeuchi, Y. Taga, *IEEE Trans. Magn.* 33 (1997) 4367.
- [12] S.Q. Xiao, Y.H. Liu, Y.Y. Dai, L. Zhang, S.X. Zhou, G.D. Liu, *J. Appl. Phys.* 85 (1999) 4127.
- [13] F. Amalou, M.A.M. Gijs, *J. Appl. Phys.* 95 (2004) 3.
- [14] Z.Y. Zhong, Z.W. Lan, H.W. Zhang, Y.L. Liu, H.C. Wang, *Acta Phys. Sin-Ch. Ed.* 50 (2001) 1610.
- [15] D. Atkinson, R.S. Beach, P.T. Squire, C.L. Platt, S.N. Hogsdon, *IEEE Trans. Magn.* 31 (1995) 3892.
- [16] H. Chiriac, T.A. Ovari, *IEEE Trans. Magn.* 38 (2002) 3057.
- [17] M. Vázquez, *J. Magn. Magn. Mater.* 226–230 (2001) 693.
- [18] D.P. Makhnovskiy, L.V. Panina, D.J. Mapps, *Phys. Rev. B* 63 (2001) 144424.
- [19] D.P. Makhnovskiy, N. Fry, L.V. Panina, D.J. Mapps, *J. Appl. Phys.* 96 (2004) 2150.
- [20] P. Allia, P. Tiberto, M. Baricco, F. Vinai, *Rev. Sci. Instrum.* 64 (1993) 1053.
- [21] C. Tannous, J. Gieraltowski, *J. Mater. Sci.-Mater. Electron.* 15 (2004) 125.
- [22] H. Chiriac, I. Murgulescu, N. Lupu, *J. Magn. Magn. Mater.* 272–276 (2004) 1860.
- [23] J. Velázquez, M. Vázquez, D.-X. Chen, A. Hernando, *Phys. Rev. B* 50 (1994) 16737.
- [24] A. Inoue, H. Koshiba, T. Itoi, A. Makino, *Appl. Phys. Lett.* 73 (1998) 744.
- [25] K. Zhang, Z. Lv, Y.Q. Liu, B. Yao, T. Zhang, B.H. Li, D.W. Zhou, B. Han, D. Wang, M. Zeng, *J. Phys. D: Appl. Phys.* 39 (2006) 4299.
- [26] R.L. Sommer, C.L. Chien, *J. Appl. Phys.* 79 (1996) 5139.
- [27] G.V. Kuryandskaya, V.M. Prida, B. Hernando, M.L. Sánchez, M. Tejedor, *Sens. Actuators A* 110 (2004) 228.
- [28] M. Kamruzzaman, I.Z. Rahman, M.A. Rahman, *J. Magn. Magn. Mater.* 262 (2003) 162.
- [29] J. He, H.Q. Guo, B.G. Shen, K.Y. He, H. Kronmüller, *J. Appl. Phys.* 86 (1999) 3873.
- [30] M. Knobel, M.L. Sánchez, C. Gomez-Polo, P. Marin, M. Vázquez, A. Hernando, *J. Appl. Phys.* 79 (1996) 1646.
- [31] B. Hernando, M.L. Sánchez, V.M. Prida, M. Tejedor, M. Vázquez, *J. Appl. Phys.* 90 (2001) 4783.
- [32] M. Vázquez, M. Knobel, M.L. Sánchez, R. Valenzuela, A.P. Zhukov, *Sens. Actuators A* 59 (1997) 20.
- [33] M. Tejedor, B. Hernando, M.L. Sánchez, V.M. Prida, *J. Magn. Magn. Mater.* 160 (1996) 311.
- [34] H. Chiriac, T.A. Óvári, C.S. Marinescu, *IEEE Trans. Magn.* 33 (1997) 3352.
- [35] X.Z. Zhou, G.H. Tu, H. Kunkel, G. Williams, *Sens. Actuators A* 125 (2006) 387.
- [36] J.P. Sinnecker, E.H.C.P. Sinnecker, A. Zhukov, J.M. Garcia-Beneytez, J.M. Garcia Prieto, M. Vázquez, *J. Phys. IV* 8 (1998), Pr2-225.